

Current Biology, Volume 21

Supplemental Information

In Vivo Optogenetic Stimulation of Neocortical Excitatory Neurons

Drives Brain-State-Dependent Inhibition

**Celine Mateo, Michael Avermann, Luc J. Gentet, Feng Zhang, Karl Deisseroth,
and Carl C.H. Petersen**

Supplemental Inventory

1. Supplemental Figures

Figure S1, related to Figure 1

Figure S2, related to Figure 2

Figure S3, related to Figure 3

Figure S4, related to Figure 4

2. Supplemental Experimental Procedures

3. Supplemental References

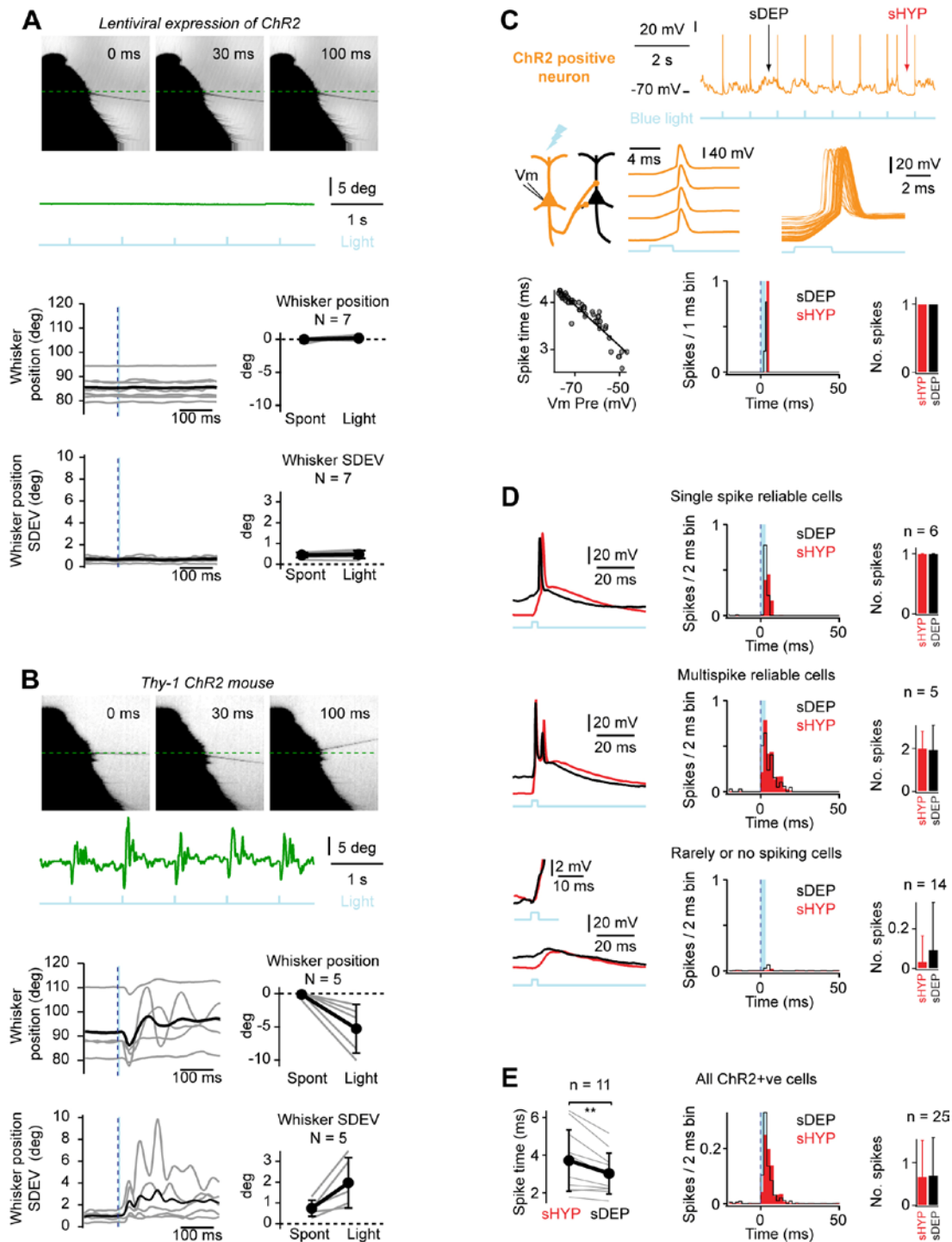


Figure S1. Optogenetic Stimulation of Excitatory Layer 2/3 Barrel Cortex Neurons Expressing ChR2 from a Lentivirus Does Not Evoke Whisker Movement, but Is Reliable across Trials and Independent of Spontaneous Cortical Activity under Our Experimental Conditions

(A) High-speed filming of the contralateral C2 whisker (*top*) in an awake head-restrained mouse following a blue light stimulus (3 ms, 1 Hz, ~ 10 mW/mm²) of layer 2/3 pyramidal neurons expressing ChR2 from a lentiviral injection targeted to the C2 barrel column. Quantification of C2 whisker position indicated that the optogenetic stimuli did not evoke whisker movement (*below*; green trace shows whisker position and light stimuli are indicated by the blue line). Averaged across many blue light

stimuli across 7 mice, the optogenetic stimulation of layer 2/3 pyramidal neurons expressing ChR2 from a lentivector did not evoke whisker movement (*left*; averages for individual mice in grey, grand average in black, light stimulation: blue line). The change in whisker position was computed comparing the whisker position during baseline and a window averaged 25 to 30 ms after the onset of the light. The data obtained with the optogenetic stimulation (*Light*) was compared to the same measures in the absence of stimulation (*Spont*). The standard deviation of whisker position was computed on sliding 30 ms time windows (individual animals in grey, grand average in black) (*left*). No difference in the standard deviation of the whisker position was found comparing between the light and the spontaneous conditions (computed from 20 to 40 ms post light stimulation and in the absence of stimulation) (*right*).

(B) Localised brief light flashes (3 ms, 1 Hz, 400 μ m optic fibre coupled to a blue LED) were delivered to the primary somatosensory barrel cortex of Thy1-ChR2 mice expressing Channelrhodopsin-2 primarily in layer 5 excitatory neurons (Jackson Laboratory strain B6.Cg-Tg(Thy1-COP4/EYFP)18Gfng/J) [49]. Each light flash (blue line) triggered a brief C2 whisker retraction [32], followed by protraction (whisker position shown in green trace). Across 5 animals a 5.3 ± 3.7 deg retraction was observed in response to light stimulation. The standard deviation of the whisker position increased in response to light stimulation. Quantification as for panel A. We conclude that the optogenetic stimulation of L5 neurons in primary somatosensory cortex of Thy1-ChR2 mice drives whisker retraction, whereas the optogenetic stimulation of a small number of lentivirus transduced L2/3 neurons expressing ChR2 does not evoke whisker movement. All data presented as mean \pm standard deviation.

(C) Whole-cell membrane potential recording of a ChR2-expressing (ChR2 +ve) layer 2/3 neuron (*upper trace*). The membrane potential of the cell fluctuated between periods of spontaneous network hyperpolarisation (sHYP, red) and periods of spontaneously depolarised cortical network activity (sDEP, black). A single action potential was reliably triggered by each and every 3 ms blue light pulse applied at 1 Hz. Spontaneous spikes were also observed. Light-flashes evoked rapid short-latency (<300 μ s) depolarisation with spikes time-locked to the light stimulation (*middle*). The latency for evoking an action potential was shorter during periods of spontaneously depolarised prestimulus membrane potentials (*lower left*). The 100% spiking probability per trial was not affected by sDEP or sHYP network states (*lower right*).

(D) In six out of 25 ChR2-expressing neurons, light evoked reliable single spikes irrespective of spontaneous sHYP or sDEP network activity (*upper*). Light evoked multiple spikes in five out of 25 ChR2-expressing cells, but their spiking probability was also not affected by the spontaneous membrane potential fluctuations (*middle*). Most ChR2-expressing neurons (14/25) did not spike in response to light or only rarely spiked in response to light (*lower*). In this population, the number of evoked spikes was very small, but the few spikes that were evoked occurred preferentially during sDEP states (black). Comparing between different neurons, light therefore evoked different numbers of action potentials in different neurons, presumably due to differences in ChR2 expression levels and to differing access of blue light to the neurons (for example due to blood vessels).

(E) Quantified across the population, light-induced spikes in ChR2-expressing neurons occurred slightly earlier during sDEP states (*left*) (spike time: 3.0 ± 1.1 ms in sDEP and 3.7 ± 1.6 ms in sHYP; $n = 11$; $P < 0.005$), but the number of evoked action potentials was not significantly modulated by spontaneous network activity (*right*) (quantified over the 10 ms after light onset: sDEP 0.69 ± 0.89 spikes; sHYP 0.66 ± 0.86 spikes; $n = 25$). The optogenetic stimulus was therefore reliable from trial to trial, independent of the level of spontaneous cortical network activity under our experimental conditions.

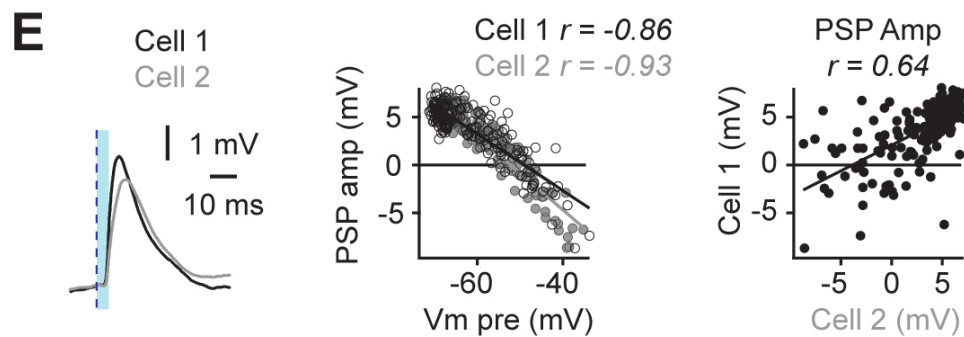
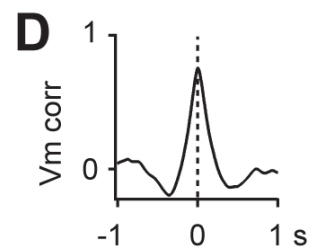
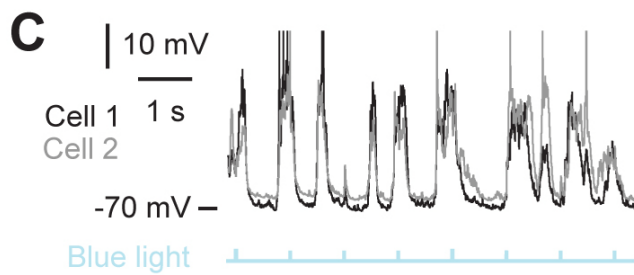
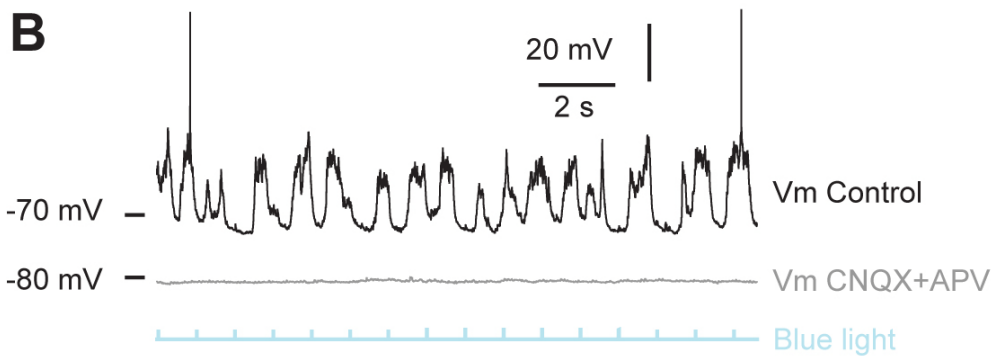
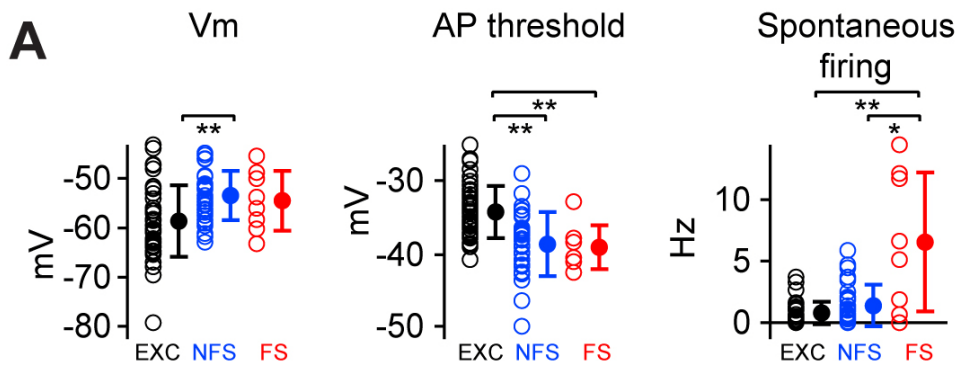


Figure S2. Cell-Type-Specific Electrophysiological Characteristics of Layer 2/3 Neurons; Dependence of Spontaneous Network Activity upon Local Glutamatergic Synaptic Transmission; and Responses to Optogenetic Stimulation in a Dual Whole-Cell Recording

(A) Mean membrane potential (V_m), action potential threshold and spontaneous firing rate for the different classes of recorded neurons. GABAergic neurons were depolarised on average compared to excitatory neurons (FS -54.5 ± 6.1 mV, $n=8$; NFS -53.4 ± 4.9 mV, $n=32$; EXC -58.6 ± 7.3 mV, $n=42$). GABAergic neurons also had lower action potential thresholds (FS -39.0 ± 3.0 mV, $n=8$; NFS -38.6 ± 4.3 mV, $n=32$; EXC -34.2 ± 3.6 mV, $n=42$). It should be noted that action potential threshold measured in awake GAD67-GFP mice does not differ comparing across the same cell types [16], and the more depolarised action potential threshold for excitatory neurons relative to inhibitory neurons found here might therefore relate to urethane anesthesia. Indeed, we found a significant ($P < 0.005$) difference in action potential threshold of excitatory layer 2/3 neurons comparing recordings carried out under urethane anesthesia (-33.4 ± 3.4 mV, $n=31$) with recordings carried out in awake mice (-36.6 ± 2.9 mV, $n=11$). FS GABAergic neurons spontaneously fired action potentials at a higher rate than NFS GABAergic neurons and excitatory neurons (FS 6.6 ± 5.6 Hz, $n=8$; NFS 1.4 ± 1.7 Hz, $n=32$; EXC 0.79 ± 0.92 Hz, $n=42$). Each open circle represents an individual neuron. Filled circles with error bars represent mean \pm SD. Statistical significance is indicated by * for $P < 0.017$ and ** for $P < 0.0017$.

(B) Whole-cell membrane potential recording (black trace, V_m) from a postsynaptic excitatory neuron showing spontaneous membrane potential fluctuations and receiving ChR2-driven synaptic inputs (blue light stimuli indicated below in blue). Both spontaneous and ChR2-evoked membrane potential fluctuations are completely blocked by application of CNQX (AMPA receptor antagonist, 0.8 mM) and APV (NMDA receptor antagonist, 1.6 mM) to the cortical surface (grey trace, V_m after application of CNQX and APV). Such blockade shows that both the spontaneous activity and the optogenetic responses depend on glutamatergic synaptic transmission.

(C) Simultaneous whole-cell recording of membrane potential from two excitatory neurons. Spontaneous membrane potential fluctuations are highly correlated in the two neurons. These two postsynaptic neurons also received synaptic inputs driven by ChR2 stimuli (blue light indicated below).

(D) Cross correlation of the membrane potentials recorded in the two neurons quantitatively revealed highly correlated membrane potential dynamics in these two nearby neurons.

(E) The ChR2-evoked PSP responses in both neurons had similar amplitudes and time-courses (*left*). In addition, the PSP amplitudes were strongly modulated in both neurons by the prestimulus membrane potential, with similar reversal potentials in both cells (*middle*). On a trial-by-trial basis the amplitude of the ChR2-evoked PSPs also covaried in both neurons (*right*).

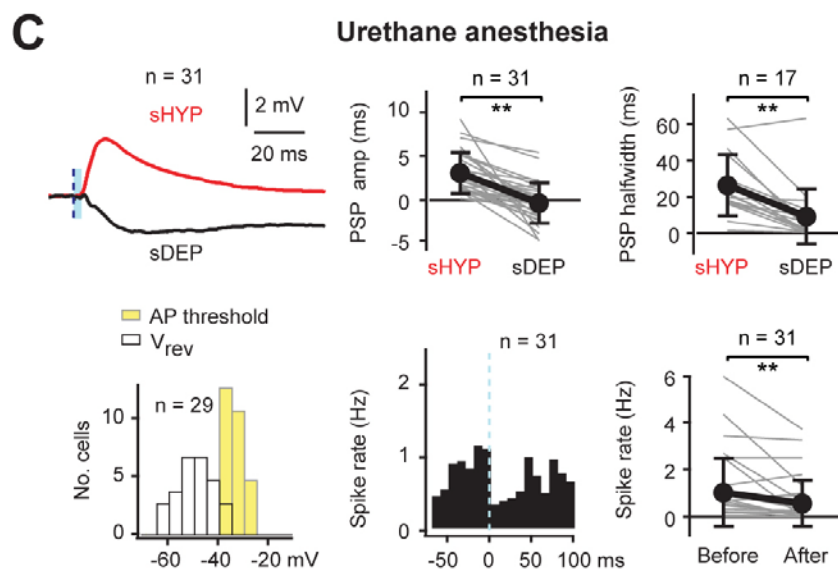
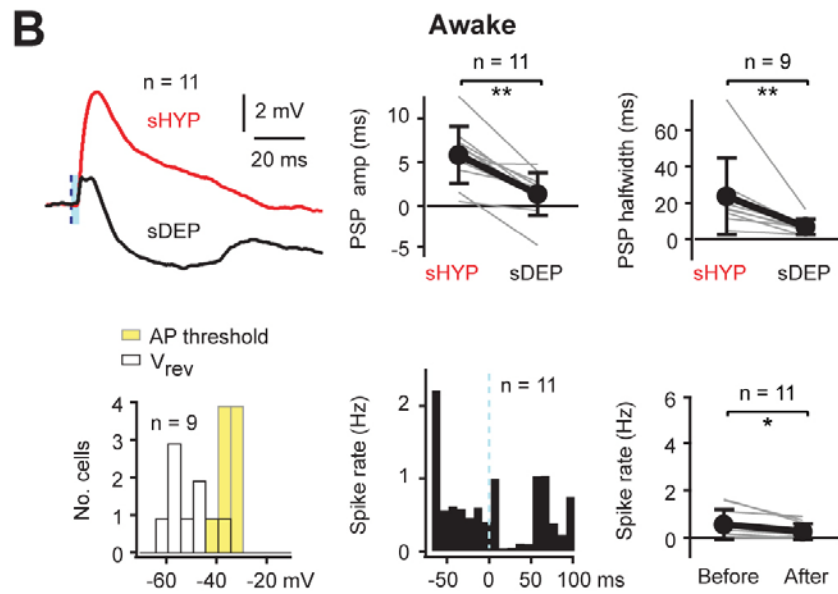
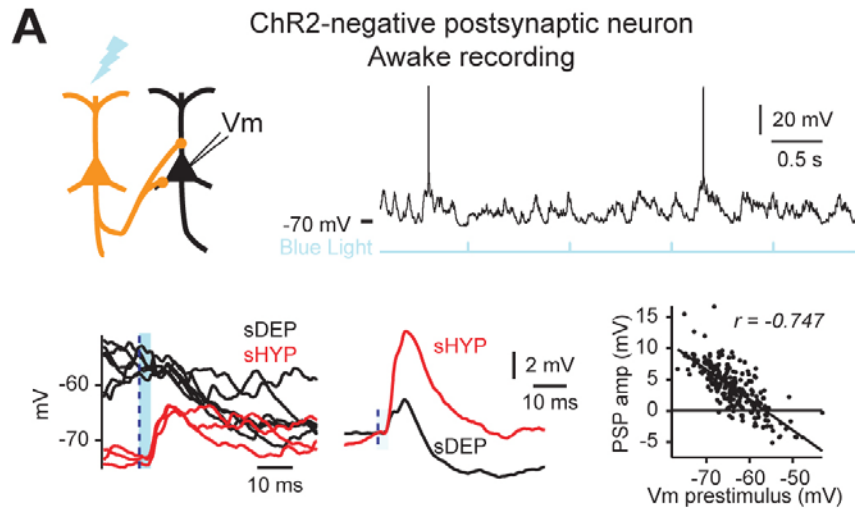


Figure S3. Comparison of ChR2-Evoked Postsynaptic Responses in Awake and Urethane-Anesthetised Mice

(A) Whole-cell recording from an awake head-restrained mouse during quiet wakefulness (black trace, V_m; blue trace, optogenetic blue light stimuli). PSPs evoked during periods of spontaneous network depolarisation (sDEP, black) were smaller in amplitude compared to PSPs evoked during periods of spontaneous network hyperpolarisation (sHYP, red). Plotting the ChR2-evoked PSP amplitude as a function of prestimulus membrane potential revealed a linear relationship in awake mice, similar to that observed in anesthetised mice.

(B and C) Group analyses of all awake recordings from postsynaptic neurons (panel B, n = 11) compared to the same analyses for recordings under urethane anesthesia (panel C, n = 31). The PSP was modulated by spontaneous network activity in a similar fashion in awake and anesthetised mice. The PSP amplitude was strongly reduced during sDEP states compared to sHYP states in both awake and anesthetised mice. The PSP duration was also strongly reduced during sDEP states compared to sHYP states in both awake and anesthetised mice. The PSP reversal potential (V_{rev}) was hyperpolarised relative to action potential threshold in both awake and anesthetised mice. The net result of the optogenetic stimulus of excitatory L2/3 pyramidal neurons in both awake and anesthetised mice was therefore to suppress action potential firing in neighbouring L2/3 pyramidal neurons. Each grey line represents an individual neuron and black circles with error bars represent mean ± SD. Statistical significance is indicated by * for $P < 0.05$ and ** for $P < 0.005$.

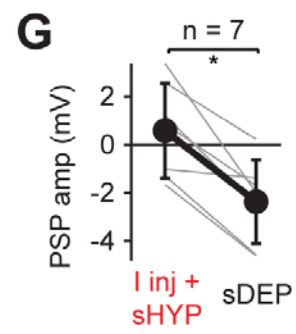
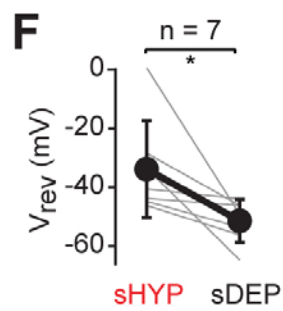
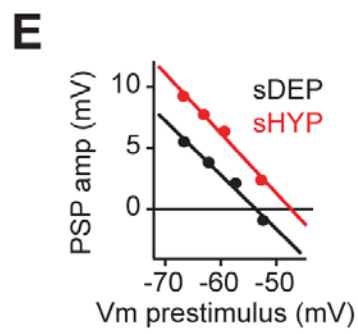
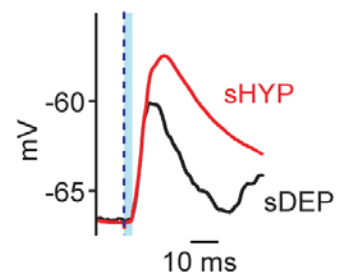
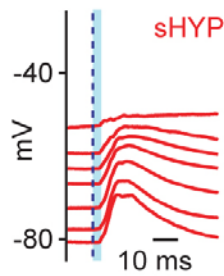
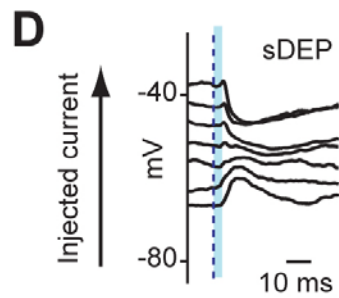
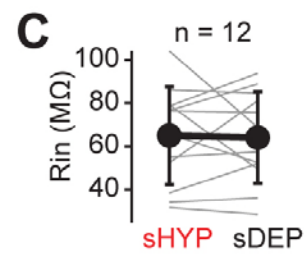
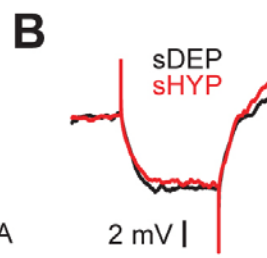
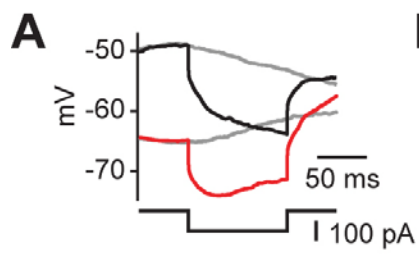


Figure S4. Effect of Spontaneous Activity upon Somatic Input Resistance and Reversal Potential of ChR2-Evoked PSPs

(A) Hyperpolarising current pulses were injected into a layer 2/3 pyramidal neuron in order to measure somatic input resistance during spontaneous activity. Average membrane potential changes evoked by injection of hyperpolarising current during periods of spontaneous network depolarisation (sDEP, black) and periods of spontaneous network hyperpolarisation (sHYP, red). Averaged spontaneous fluctuations in the absence of current injection are superimposed in grey.

(B) Spontaneous fluctuations were then subtracted from the average responses to current injection and access resistance was corrected. Somatic input resistance in this recording did not change comparing between sHYP and sDEP cortical network states.

(C) Population data across 12 cells shows no significant modulation of the somatic input resistance (R_{in}) comparing sHYP states and sDEP states (R_{in} : $64.1 \pm 21.2 \text{ M}\Omega$ in sDEP and $64.9 \pm 22.7 \text{ M}\Omega$ in sHYP). Under our experimental conditions, changes in somatic input resistance during spontaneous network activity therefore do not appear to contribute to the differences in postsynaptic responses evoked by the optogenetic stimulus.

(D) Different amounts of current were injected through the whole-cell recording electrode in order to examine the cell-autonomous effect of postsynaptic membrane potential upon the light-evoked response. The amplitude of the light-evoked response decreased upon depolarisation. At a given postsynaptic membrane potential, the light-evoked response was larger during periods of spontaneous network hyperpolarisation (sHYP, red) than during periods of spontaneous network depolarisation (sDEP, black) (*right*).

(E) For the same recording, the amplitude of light-evoked responses during sDEP states (black) and sHYP states (red) versus prestimulus membrane potential varied through current injections.

(F) Quantified across 7 cells, the reversal potential of the postsynaptic responses was more hyperpolarised during sDEP states compared to during sHYP cortical states (V_{rev} sDEP = $-51.4 \pm 7.3 \text{ mV}$; V_{rev} sHYP = $-33.8 \pm 16.5 \text{ mV}$; $n = 7$; $P = 0.016$). This suggests enhanced recruitment of inhibitory neurons by the optogenetic stimulation of excitatory neurons during spontaneously depolarised periods of cortical network activity. Each grey line represents an individual neuron and black circles with error bars represent mean \pm SD. Statistical significance is indicated by * for $P < 0.05$.

(G) Light stimuli were delivered during a period of spontaneous hyperpolarisation whilst depolarising current was injected (I_{inj} sHYP) to bring the membrane potential to the same value as that of the spontaneous depolarised (sDEP) network state. The PSP amplitudes during I_{inj} sHYP were significantly larger than PSP amplitudes during sDEP states. Each grey line represents an individual neuron and black circles with error bars represent mean \pm SD. Statistical significance is indicated by * for $P < 0.05$.

Supplemental Experimental Procedures

All experiments were carried out in accordance with the Swiss Federal Veterinary Office.

Animal Preparation and Surgery

C57BL6J and GAD67-GFP mice [33], 3-5 weeks old, were implanted with a light-weight metal head-holder and a recording chamber under deep isoflurane anesthesia [16,19,21,35]. All whiskers except C2 were trimmed and the location of left C2 barrel column was functionally located through intrinsic optical imaging under light isoflurane anesthesia [30]. The cortical surface was visualised through the intact bone. The C2 whisker was deflected at 10 Hz for 4 s and the evoked hemodynamic signal was imaged by a Qicam CCD camera (Q-imaging) under 630 nm illumination provided by LEDs. The images were processed online by custom written routines running in IgorPro (Wavemetrics). A small craniotomy was made over the functionally identified location of the C2 barrel column to target lentiviral injections and whole-cell recordings.

Lentivirus injection

Lentivirus pressure injections were performed in layer 2/3 of the C2 barrel column under deep isoflurane anesthesia [30]. A small volume (~50 nl) of lentivirus (10^7 IU/mL) encoding ChR2-YFP driven by the α CaMKII promoter [27] was injected with a thin glass pipette (tip diameter ~10 μ m). *In vivo* whole-cell recordings were made after allowing at least 4 weeks for sufficient and stable expression of ChR2.

Electrophysiology

Whole-cell membrane potential recordings were made in the C2 barrel column of mice under urethane anesthesia (1.7 mg/g) maintained at 37°C with a heating blanket. In addition, a small number of experiments were carried out in awake head-restrained mice. Mice readily habituate to head-restraint. The first head-restrained sessions of each mouse lasted only for a few minutes and this period was gradually increased each day until the mouse would sit calmly for a period of roughly one hour. Following several days of habituation to head-restraint, recordings were performed in a session lasting up to 2 hours.

Patch pipettes (4-7 M Ω resistance) were filled with a solution containing (in mM): 135 potassium gluconate, 4 KCl, 10 HEPES, 10 Na₂Phosphocreatine, 4 MgATP, 0.3 Na₃GTP (adjusted to pH 7.3 with KOH), and 3 mg/ml biocytin for *post hoc* anatomical identification. For two-photon targeted recordings, 10 μ M Alexa 594 (Invitrogen) was added to the pipette solution [16]. GFP-expressing GABAergic neurons were visualised using a two-photon laser scanning microscope (Prairie Instruments). Femtosecond pulsed infrared excitation light of 880 nm was generated by a MaiTai laser (SpectraPhysics) and focused into the brain via a 40x 0.8NA water immersion objective (Olympus). Backscattered infrared light was prevented from hitting the photomultiplier tubes (PMTs) by an E650SP filter (Chroma Technology). A dichroic mirror followed by bandpass filters split emitted fluorescence into a red (607 \pm 22.5 nm) PMT channel and a green (525 \pm 35 nm) PMT channel. Whole-cell electrophysiological measurements were made with Multiclamp 700 amplifiers (Axon Instruments). The membrane potential was filtered at 10 kHz and digitised at 20 kHz by an ITC-18 (Instrutech Corporation) under the control of IgorPro. The membrane potential was not corrected for liquid junction potentials. Only cells in supragranular layers were analysed (subpial depth < 450 μ m). A superbright LED (Luxeon, Philips) generated blue light flashes, which were focused onto the cortex (3 ms, 1 Hz, 470 nm, ~10 mW/mm²). After the experiments, the mice were perfused with 4%

paraformaldehyde (PFA) and, subsequently, brains were sliced coronally. Biocytin staining with Streptavidin Alexa Fluor 594 conjugate (Invitrogen) and GFP antibody staining (Ab290, Abcam, Cambridge, UK) were performed to reveal the morphology of the recorded neurons and the lentivirus-mediated ChR2-YFP expression.

Data Analysis

All data are presented as mean \pm standard deviation. Statistical analysis was performed in IgorPro. Nonparametric statistical tests were used to assess significance (Wilcoxon-Mann-Whitney two-sample rank test or Wilcoxon Signed Rank test). For multiple comparisons between excitatory, FS GABAergic and NFS GABAergic neurons, significance was assessed after Bonferroni correction ($P < 0.017$) using the Wilcoxon-Mann-Whitney two-sample rank test. The linear relationship between two variables was tested using *Pearson's* linear correlation test. The number of cells analysed is denoted by 'n'. P values were presented as * for $P < 0.05$ (or $P < 0.05/3$ for multiple comparison after Bonferroni correction) and ** for $P < 0.005$ (or $P < 0.005/3$ for multiple comparison after Bonferroni correction).

Light-induced responses were separated according to the membrane potential prior to the optogenetic stimulus into 2 categories: sHYP (spontaneously hyperpolarised) and sDEP (spontaneously depolarised). The sHYP state was defined to include all trials in which the mean membrane potential 20 ms prior to light stimuli was within 5 mV of the most hyperpolarised membrane potential observed in the recording of the given neuron. The sDEP state included all trials in which the prestimulus membrane potential was more than 10 mV depolarised compared to the most hyperpolarised membrane potential observed in the recording of the given neuron. Light stimuli delivered at intermediate prestimulus membrane potentials consistently evoked responses in between those observed during sDEP and sHYP states. In order to correct for spontaneous changes in membrane potential, the same separation of trials was computed in the absence of light stimuli. Averaged sDEP and sHYP trials without light stimuli were subtracted from the corresponding sDEP and sHYP light-induced responses. The amplitudes of the subthreshold PSP responses to light were determined by averaging the values within a 2 ms window centred around the peaktime of the average response (across all trials) and subtracting the 2 ms window prior to the start of the response (the prestimulus membrane potential). Light-evoked PSP amplitudes were linearly fitted against the corresponding prestimulus membrane potentials. The spontaneously driven reversal potential was calculated from the resulting linear fit. State dependent light-evoked postsynaptic action potential firing was computed by subtracting the spontaneous action potential firing (computed over the same duration for trials without stimulation but otherwise selected in an identical manner according to the prestimulus membrane potential for sDEP or sHYP states).

For experiments involving current injection, access resistance was compensated offline. The membrane potential was fitted exponentially from 2 ms to 50 ms after the onset of the current injection to determine and subtract the early fast component due to access resistance. Input resistance values were calculated as the difference in the mean membrane potential between two 20 ms periods, one immediately before current injection and the other 80 ms after the beginning of current injection, at which time a steady state had been reached.

Supplemental Reference

49. Arenkiel, B.R., Peca, J., Davison, I.G., Feliciano, C., Deisseroth, K., Augustine, G.J., Ehlers, M.D., and Feng, G. (2007). In vivo light-induced activation of neural circuitry in transgenic mice expressing channelrhodopsin-2. *Neuron* 54, 205-218.